第36卷第10期 无 机 化 学 学 报 Vol.36 No.10
2020年10月 CHINESE JOURNAL OF INORGANIC CHEMISTRY 1988-1996

异硫氰酸荧光素后修饰的金属有机三元环光解水制氢

张文言 杨 阳 黄慧琳 景 旭* 段春迎
(大连理工大学张大煜学院,大连 116024)

摘要: 将具有N、O、P三齿配位点的直线型双臂席夫碱配体L1与钴离子配位自组装得到一例[3+3]金属-有机三元环Co-L1。在该配体的苯环侧链上引入易于修饰的NH_2基团,通过组装后修饰的方法把光活性的异硫氰酸荧光素(FITC)分子以共价键方式键合到金属-有机三元环上,并将其用于可见光下的光解水制氢。该体系属于无须引入额外光敏剂的双组分放氢体系。与传统的三组分体系相比,在同等金属催化剂和光敏剂浓度下,组装后修饰的金属配合物催化剂Co-L3具有更高的光催化活性,转换数(TON)可以达到80,大约是Co-L1光催化效率的30倍。

关键词: 金属有机大环; 钴; 光催化产氢; 组装后修饰
中图分类号: O614.81+2 **文献标识码:** A **文章编号:** 1001-4861(2020)10-1988-09
DOI: 10.11862/CJIC.2020.206

Photocatalytic Hydrogen Production Based on Metal-Organic Triangle Modified by Fluorescein Isothiocyanate

ZHANG Wen-Yan YANG-Yang HUANG Hui-Lin JING Xu* DUAN Chun-Ying
(*Zhang Dayu School of Chemistry, Dalian University of Technology, Dalian, Liaoning* 116024, *China*)

Abstract: A cobalt based metal-organic [3+3] self-assembly macrocycle was constructed by tridentate Schiff base ligand L1 with N, O and P atoms (L1=1,1′-biphenyl-4,4′-di-carbohydrazide-bis-(2-diphenyphosphinobenzaldehyde)). The functionalized metal-organic triangle with amino groups was connected to photoactive fluorescein isothiocyanate (FITC) via post-assembly modification reaction. This modified complex Co-L3 was used as photocatalyst for hydrogen evolution from water splitting. It was a two-component system for hydrogen production without extra photosensitizer. Besides, compared with the three-component system, the metallosupramolecular catalyst Co-L3 underwent post-assembly modification reactions exhibited higher photocatalytic activity at the same metal catalyst and photosensitizer concentration with a turnover number (TON) of 80, which was approximately 30 times the photocatalytic efficiency of complex Co-L1.

Keywords: metal-organic macrocycle; cobalt; light-driven H_2 production; post-assembly modification

0 Introduction

Hydrogen (H_2) gas acquires a high combustion calorific value and only produces water during combustion, so it is considered as an alternative, sustainable and clean energy[1]. Artificial photosynthetic H_2 production is regarded as an effective way to convert and utilize solar energy. Building an efficient, low-cost, nontoxic and chemically stable photocatalytic system is a goal that scientists have always pursued. The current research mainly focuses on the three aspects of photocatalytic hydrogen production semi-reaction[2], visible

收稿日期:2020-05-19。收修改稿日期:2020-06-17。
国家自然科学基金(No.21971030)和大连理工大学基本科研业务费(No.DUT20ZD218)资助项目。
*通信联系人。E-mail:xjing@dlut.edu.cn

light-driven hydrogen decomposition[3-5] and hydrogen production coupled with visible light catalysis organic conversion[6-9]. At present, scientists have developed artificial photocatalytic systems for the generation of hydrogen from water based on molecular photosensitizers (such as eosin, fluorescein and metal complexes)[10-18] and semiconductor light-capturing materials (such as TiO_2, C_3N_4 and CdS)[19-21]. The efficiency and stability of photocatalytic hydrogen production have been continuously improved.

The metal-organic supramolecular complexes with nanoscopic size and well-defined hydrophobic cavities are regarded as mimics of natural photocatalytic system by catching organic dyes in their pockets[22-27]. Compared to other relevant systems, these supramolecular architectures are superior in light-driven hydrogen production by enhancing the proximity between the photosensitizer and the catalytic center and increasing the effective local concentration of the substrates within the container[24].

However, host-guest supramolecular system requires a large excess of photosensitizers for hydrogen evolution[28]. It is mainly due to the poor stability of the photosensitizer and the weak and dynamic host-guest interaction. So, we developed a post-assembly modification strategy by connecting quantitative photosensitizer fluorescein isothiocyanate (FITC) to metal-organic complex in order to improve the stability of photosensitizer. Compared to traditional three-component hydrogen production system, it was a two-component system consisting of catalyst and electron sacrificial agent. We firstly synthesized the Schiff base ligand L1 and corresponding metal-organic triangles Co-L1. Therefore, the functionalized metal-organic triangles Co-L3 were constructed by complex Co-L2 with amino groups which could be easily bonded to photoactive FITC units. The photocatalytic activity of catalyst Co-L3 in two-component system was higher than that of Co-L1 in three-component system under the same reaction conditions. This post-assembly modification strategy provides a novel idea for metal-organic confined supramolecular.

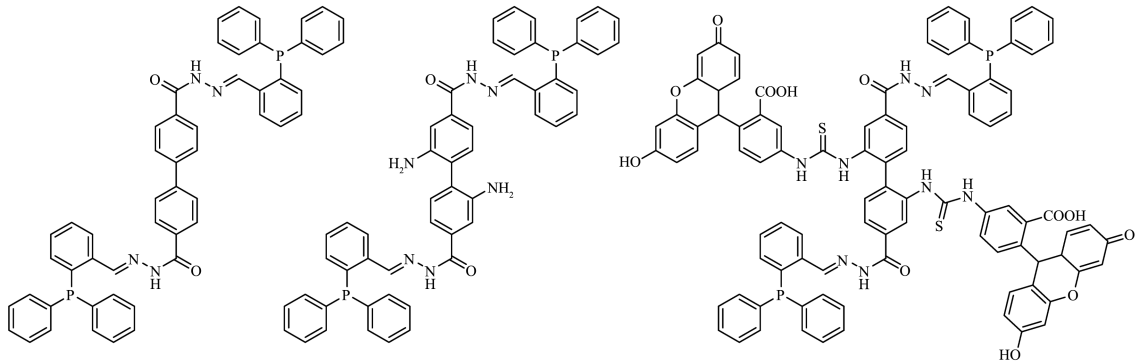

Fig.1　Structures of ligands L1, L2 and L3

1　Experimental

1.1　Materials and instruments

All reactions were carried out under N_2 atmosphere with standard Schlenk techniques. Solvents were dried and distilled prior to use according to the standard methods. All chemicals were of reagent grade obtained from commercial sources and used without further purification. ^{1}H NMR spectra were run on a Bruker-400 spectrometer with tetramethylsilane (^{1}H) as an internal standard. The elemental analyses of C, H and N were performed on a Vario EL Ⅲ elemental analyzer. ^{1}H NMR spectra were measured on a Varian INOVA 400M spectrometer. Electrospray ionization mass spectra (ESI-MS) were obtained on a HPLC-Q-Tof MS spectrometer. The fluorescent spectra were measured on a JASCO FP-6500.

Electrochemical measurements: Electrochemical measurements were carried out under nitrogen at room temperature on ZAHNER ENNIUM electro-chemical workstation with a conventional three-electrode system

with a homemade Ag/AgCl electrode as the reference electrode, a platinum silk with 0.5 mm diameter as the counter electrode, and a glassy carbon electrode as the working electrode. Cyclic voltammograms were obtained with the solution concentrations of 1 mmol·L^{-1} for the cobalt-based complexes and 0.1 mol·L^{-1} for the supporting electrolyte. The addition of 0.1 mmol·L^{-1} NEt_3HCl in dimethyl Formamide (DMF) was carried out with syringe.

Fluorescence quenching experiments: A solution (2.0 mL) of fluorescein (Fl) at 10 μmol·L^{-1} concentration in a EtOH/H_2O solution (1∶1, *V*/*V*, pH=12) was prepared in a quartz cuvette fitted with a septum cap, and the solution was degassed under N_2 for 15 min. Aliquots of 20 μL (1 mmol·L^{-1}) of the catalysts Co-L1 were added, and the intensity of the fluorescence was monitored by steady state fluorescence excited at 460 nm on a Spex-Fluoromax-P fluorimeter with a photomultiplier tube detector. Both excitation and emission slit widths were 2 nm.

UV-Vis absorption spectra: the cobalt-based complexes and FITC were prepared at concentration of 10 μmol·L^{-1} in DMF solution. Adding 2 mL of DMF in each of the two wide quartz cuvettes in order to eliminate background interference, then above solutions were gradually added into one of the two quartz cuvettes by a micro-syringe. Solutions were stirred evenly and stood for 3 min. Test range of UV-Vis absorption spectrum was set to 250~700 nm.

Photocatalytic proton reduction experiments: photoinduced hydrogen evolution was performed in a 20 mL flask. Varying amounts of the catalysts, Fl and NEt_3 in EtOH/H_2O (1∶1, *V*/*V*) were added to obtain a total volume of 5.0 mL. The flask was sealed with a septum and degassed by bubbling argon for 15 min. The pH of this solution was adjusted to a specific pH by adding HCl or NaOH and measured with a pH meter. The samples were irradiated by a 500 W Xenon lamp with the light filter (<420 nm), and the reaction temperature was maintained at 293 K by using a thermostat water bath. The generated H_2 was characterized by GC 7890T instrument analysis using a 0.5 nm molecular sieve column (0.6 m×3 mm), thermal conductivity detector, and argon used as carrier gas. The amount of hydrogen generated was determined by the external standard method.

1.2 Syntheses of L1 and L2

Ligand L1: the ligand L1 was synthesized by adding dimethyl biphenyl-4,4-dicarboxylate (10 mmol, 2.7 g) and hydrazine monohydrate (40 mL) into a round bottomed flask. After heating at 70 ℃ for 24 hours, the mixture was cooled to room temperature and then washed thoroughly with methanol to remove excess hydrazine hydrate. The above product (5 mmol, 1.35 g) was mixed with 150 mL ethanol in a 250 mL round bottom flask, and then 0.25 mL AcOH was added dropwise. After refluxing for 12 h, the mixture was filtered while hot and washed with hot methanol. Yield: ~90%. Anal. Calcd. for $C_{52}H_{40}N_4O_2P_2$(%): C, 76.65; H, 4.95; N, 6.88. Found (%): C, 76.29; H, 5.02; N, 6.88. ^{1}H NMR (400 MHz, DMSO-d_6): δ 12.06 (s, 2H), 9.22 (s, 2H), 8.17~7.79 (m, 12H), 7.43 (s, 14H), 7.24 (s, 6H), 6.88 (s, 2H).

Ligand L2: dimethyl phthalate (1.00 g, 3.7 mmol) was added into concentrated H_2SO_4 (10 mL, 98%) and stirred at room temperature for 10 min. Nitric acid (760 μL, 65%) was added to a concentrated H_2SO_4 (2 mL) to obtain a mixed acid, which was slowly added dropwise to the above solution. The mixture was stirred for 4 hours under ice bath, and then poured into ice (300 mL) to give a beige solid. Then beige solid (10.3 g, 0.03 mol) was dissolved in 300 mL of acetic acid and iron powder (18.2 g, 0.32 mol) was added. The mixture was stirred at 50 ℃ for 14 h. The suspension was filtered, and the filtrate was partly dried in vacuum. After washing with saturated aqueous sodium hydrogen carbonate, the solution was extracted with CH_2Cl_2. The combined organic layers were dried under vacuum and recrystallized in CH_2Cl_2 for purification. The above intermediate (1.5 g, 5 mmol), 2-diphenylphosphinobenzaldehyde (3.2 g, 11 mmol) and ethanol (150 mL) were added into a 250 mL round bottom flask, and the mixture was refluxed for 12 h. After completion of the reaction, the mixture was filtered while hot, washed with hot methanol and then evaporated to dryness. Yield: ~70%. Anal. Calcd. for $C_{52}H_{42}N_6O_2P_2$(%): C,

73.92; H, 5.01; N, 9.95. Found (%): C, 73.06; H, 5.07; N, 10.10. ^{1}H NMR (400 MHz, DMSO-d_6): δ 11.94 (s, 2H), 9.19 (s, 2H), 8.09 (s, 2H), 7.43 (s, 18H), 7.32 (s, 2H), 7.23 (s, 10H), 7.08 (s, 2H), 6.84 (s, 2H), 4.94 (s, 4H).

1.3 Syntheses of complexes Co-L1, Co-L2 and Co-L3

Co-L1: the ligand L1 (0.1 mmol, 0.082 g) and Co$(ClO_4)_2\cdot 6H_2O$ (0.12 mmol, 0.031 g) were dissolved in 20 mL methanol. After refluxing for 6 h, the red mixture was filtered. The red block crystals were obtained by slow evaporation of the solvent in two weeks under room temperature. Yield: ~55%. Anal. Calcd. for $C_{156}H_{120}N_{12}O_6P_6Co_3$(%): C, 69.26; H, 4.47; N, 9.32. Found(%): C, 69.28; H, 4.49; N, 9.12. ESI-MS *m/z*: $[3Co+3L1-6H]^{3+}$, 871.513 5; $[3Co+3L1-6H+ClO_4]^{2+}$, 1 357.244 5.

Co-L2: the synthesis of complex Co-L2 was similar to Co-L1 with the ligand L2 (0.1 mmol, 0.085 g) and $Co(ClO_4)_2\cdot 6H_2O$ (0.12 mmol, 0.031 g). After several days, red block crystals were obtained. Yield: ~35%. Anal. Calcd. for $C_{156}H_{126}N_{18}O_6P_6Co_3$(%): C, 69.10; H, 4.68; N, 9.30. Found(%): C, 69.20; H, 4.65; N, 9.31. ESI-MS *m/z*: $[3Co+3L2-6H]^{3+}$, 901.552 7; $[3Co+3L2-6H+ClO_4]^{2+}$, 1 402.302 1.

Co-L3: the FITC (0.7 mmol, 29 mg) was dissolved in 10 mL DMF, and then added dropwise to the DMF solution of Co-L2 (0.1 mmol, 28 mg). The mixture was stirred at room temperature for 24 h. The solution was evaporated in vacuo and excess FITC was removed with ethanol. The red block crystals were obtained in two weeks under room temperature. Yield: ~40%. ESI-MS *m/z*: $[3Co+3L2-6H+3FITC]^{3+}$, 1 290.903 1; $[3Co+3L2-6H+4FITC]^{3+}$, 1 420.913; $[3Co+3L2-6H+5FITC]^{3+}$, 1 550.953 1; $[3Co+3L2-6H+6FITC]^{3+}$, 1 680.271 2.

2 Results and discussion

2.1 ESI-MS spectra of Co-complexes

The ESI-MS spectrum of Co-L1 in DMF solution demonstrated the stoichiometry of the formation of metal-organic triangles (Fig.2a). Isotopically resolved peaks corresponding to the intact and discrete [3+3] assembly complex Co-L1 was observed at *m/z*=871.513 5 and 1 357.244 5 which are assigned to the $[3Co+3L1-6H]^{3+}$ and $[3Co+3L1-6H+ClO_4]^{2+}$, further providing convincing evidence for the existence of the metallacycle as the only supramolecular species and its stability in DMF solution. Moreover, six hydrogen atoms lost in the entire supramolecular species were derived from the active hydrogen atoms in the hydrazide, which also illustrated the coordination mode of metal ions and ligands.

The cobalt centers in complex Co-L2 possessed the same coordination environments as those in Co-L1 (Fig.2b). Besides, free amino groups were not involved in coordination, which provided possibilities for the post-assembly modification of FITC.

As shown in Fig.2c, the Co-L3 generated peaks at *m/z* of 1 290.903 1, 1 420.913 6, 1 550.593 1 and 1 680.271 2, corresponding to $[3Co+3L2-6H+3FITC]^{3+}$, $[3Co+3L2-6H+4FITC]^{3+}$, $[3Co+3L2-6H+5FITC]^{3+}$ and $[3Co+3L2-6H+6FITC]^{3+}$, respectively. The hexafunctionalized metallacycle Co-L3 could be seen as the major product of the reaction when analyzed in conjunction with the ^{1}H NMR spectra.

2.2 Structural description for metallacycle Co-L1

It was a pity that we have not obtained good single crystal diffraction date of Co-L1 because of its poor crystallinity. The composition of Co-L1 was revealed by the ESI-MS spectrum, where signals (*m/z*) at 871.513 5 and 1 357.244 5 could be classified as $[3Co+3L1-6H]^{3+}$ and $[3Co+3L1-6H+ClO_4]^{2+}$. Each of the isotope patterns is in accord with the calculated ones. The metallacycle of Co-L1 could be seen as a M3L3 triangle consisting of three cobalt ions as vertices and three ligands as sides (Fig.3). The cobalt ions were located on two edges with an average distance of 1.5 nm and the angle between ligand and ligand was 60°. In the structure, the cobalt atoms coordinated to the two N atoms, two O atoms and two P atoms, which is similar to the octahedral configuration.

2.3 ^{1}H NMR spectra of Co-complexes

^{1}H NMR spectra of the reaction products further supported the structural information about the metallacycles. The shift of H5 (-NH_2, δ=4.9) was observed in the spectrum of Co-L2 (Fig.4), further demonstrating that free NH_2 groups were not involved in coordination.

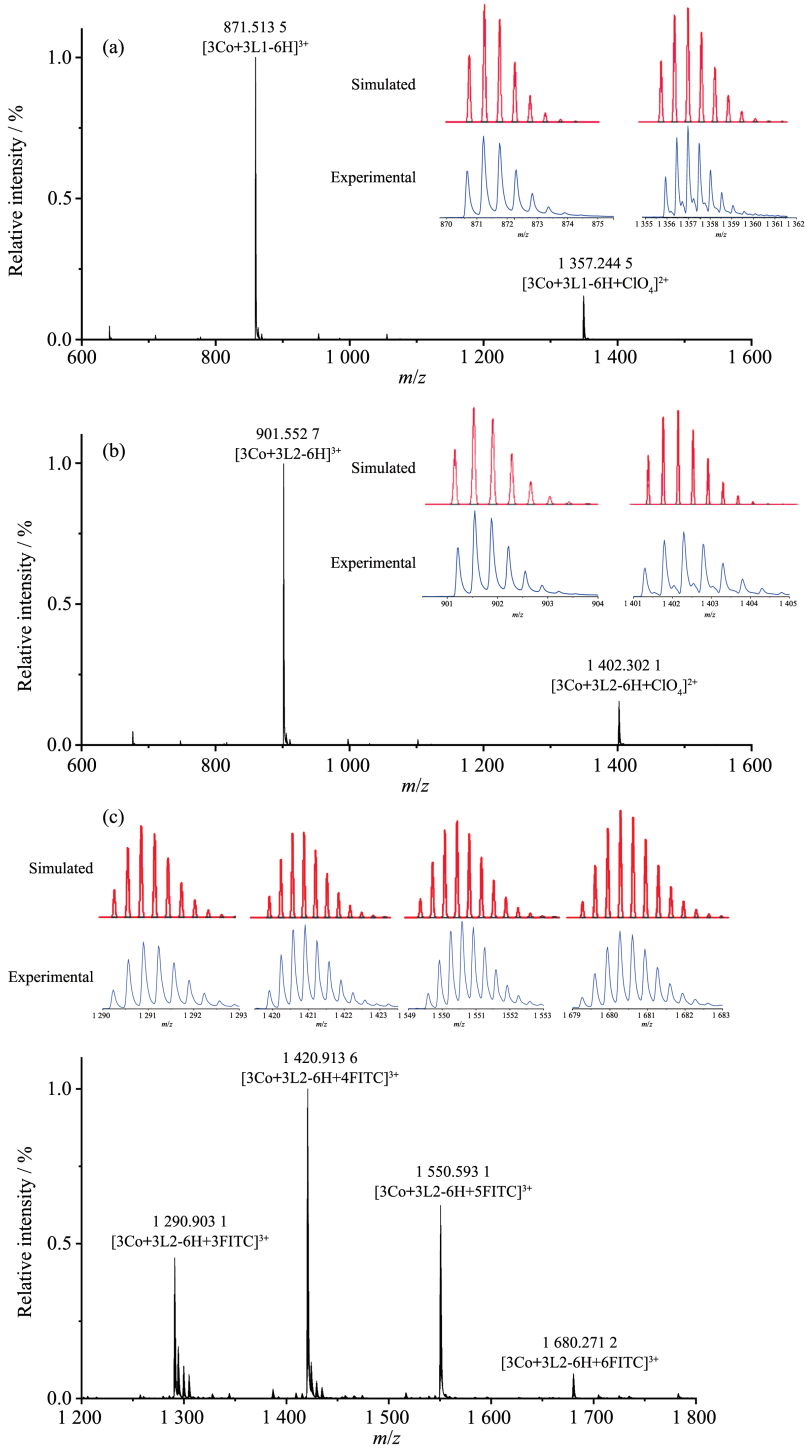

Fig.2 ESI-MS spectra of metallacycle (a) Co-L1, (b) Co-L2 and (c) Co-L3

Despite the complexity, features characteristic of Co-L3 could be identified in ^{1}H NMR spectra. Compared to the spectrum of Co-L2, we could infer that amino groups and isothiocyanate groups reacted in a ratio of 1∶1 due to the disappearance of shift of H5 (-NH_2, δ=4.9). And integration of the peaks (H1 and H4) in this spectrum also demonstrated that six FITC units were present in each metallacycle of Co-L3 on average. Both ^{1}H NMR and ESI-MS spectra provided evidence that FITC units were successfully connected to the metal-organic triangles in a covalent post-assembly modification reaction.

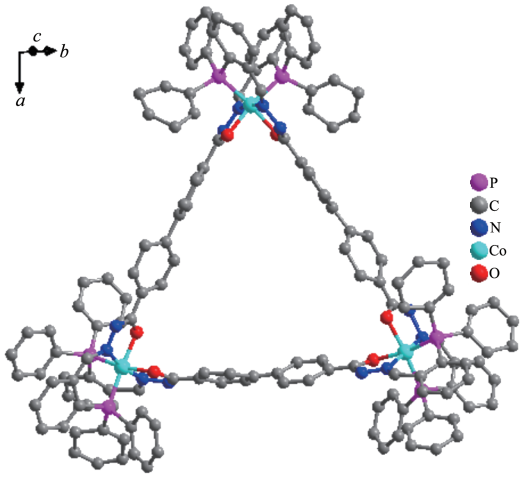

Fig.3　Schematic representation of the metal-organic triangle Co-L1 showing the coordination geometry of the cobalt ions

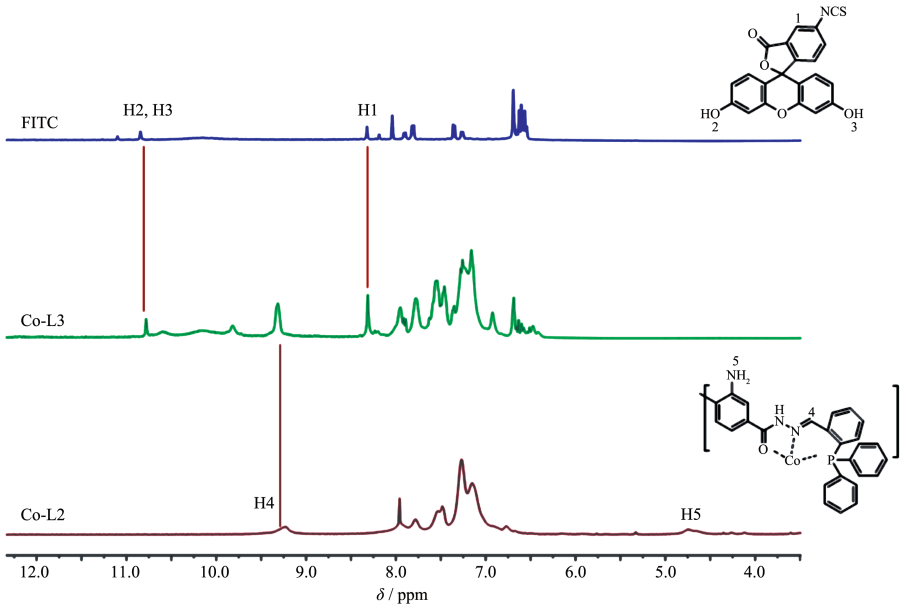

Fig.4　Partial ^{1}H NMR spectra of FITC, Co-L3 and Co-L2

2.4　Cyclic voltammetry of Co-L3

The cyclic voltammetry of Co-L3 showed that the reduction potentials of $Co^{Ⅱ}/Co^{Ⅰ}$ and $Co^{Ⅲ}/Co^{Ⅱ}$ occurred at −1.14 and −0.31 V (Fig.5a). This reduction potential of $Co^{Ⅱ}/Co^{Ⅰ}$ was more negative than the reduction potential of the proton, suggesting that Co-L3 was able to reduce proton hydrogen evolution under electrochemical conditions. To investigate the role of the Co-L3 as a proton reduction catalyst, cyclic voltammetry was performed in the presence of increasing amounts of NEt_3HCl (Fig.5b). It was found that a new proton reduction peak was induced near the reduction peak of $Co^{Ⅱ}/Co^{Ⅰ}$. This result could be regarded as the electrochemical reduction process of protons in solution, indicating that Co-L3 can reduce the proton with a catalysis process.

2.5　Co-L1 as quencher for the photosensitizer Fl

As a proton reducing agent, Co-L1 could obtain electrons from the activator in an excited state, and the actinic agent in the excited state reached a steady state usually accompanied by a decrease in the intensity of the photosensitizer emission. As shown in Fig. 6, the addition of an equivalent molar ratio of Co-L1 to an $EtOH/H_2O$ solution containing Fl obviously quenched the emission intensity, which proved possibilities for Fl to activate Co-complexes for the production of H_2. The Stern-Volmer quenching constant K_{svl} in this system

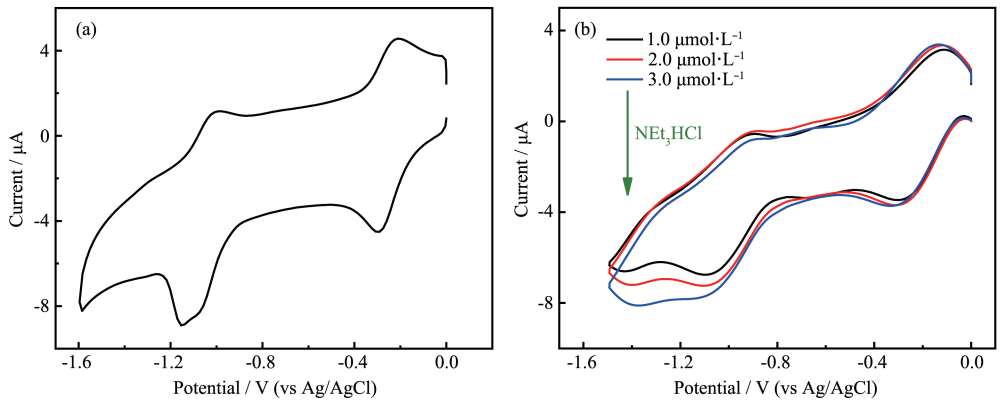

Scan rate: 100 mV·s^{-1}

Fig.5 (a) Cyclic voltammetry curve of Co-L3 (1.0 mmol·L^{-1}); (b) Cyclic voltammetry curves of Co-L3 (1.0 mmol·L^{-1}) upon addition of NEt_3HCl with different concentrations

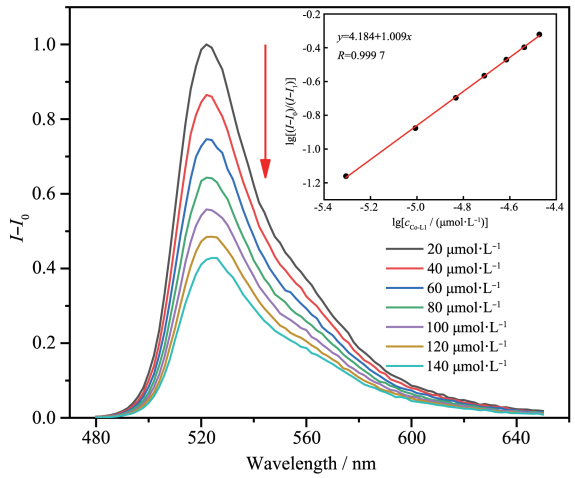

Inset: Stern-Volmer plot for the photoluminescence quenching of Fl by catalyst Co-L1

Fig.6 Emission spectra of Fl solution (10 μmol·L^{-1}) in an EtOH/H_2O (1∶1, *V*/*V*) solution upon addition of Co-L1 (1 mmol·L^{-1}) with various concentrations

was calculated as 1.51×10^4. The result showed that the complex Co-L1 could not only realize the process of electrochemical decomposition of water for hydrogen evolution, but also transferred the absorbed light energy to the redox catalyst through the excited state of fluorescein after the sensitization of fluorescein.

2.6 Photophysical properties of Co-L3

The factors that provide Co-L3 with photoactivity and stability were investigated based on the light absorbance and structural stability. Usually, cationic metal-organic macrocycles or cages constructed by Schiff base ligands have non-fluorescent emission due to intramolecular photoinduced electron transfer (PET) between luminophores and electron-deficient units. However, Co-L3 exhibited certain photophysical properties in various solvent systems despite of reduced fluorescence intensity due to interference from metal ions (Fig.7a). The light absorbances of Co-L3, Co-L1 and FITC were compared via UV-Vis spectrometry. The

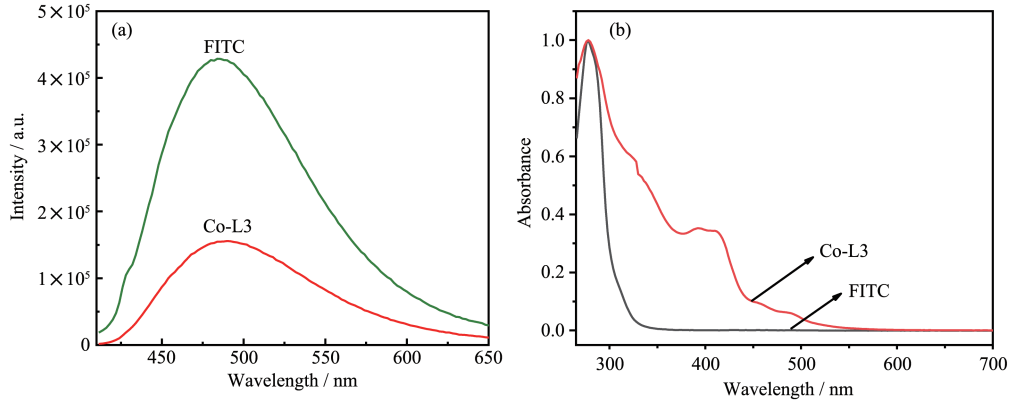

Fig.7 (a) Fluorescence spectra of FITC and Co-L3; (b) UV-Vis spectra of FITC and Co-L3

same number of FITC units were prepared in each sample, and the corresponding absorptions in the wavelength range from 260 to 700 nm were compared. As shown in Fig. 7b, the complex Co-L3 modified with FITC units showed higher light absorption, indicating that the discrete metal-organic triangles of Co-L3 improved the light absorption in the solution.

2.7 Catalytic behavior of Co-L1 and Co-L3 in H_2 evolution

Proton reduction catalytic activity of Co-L3 was evaluated in an EtOH/H_2O (1∶1, *V*/*V*) solvent mixture irradiated with visible light (λ >420 nm) containing NEt_3 as an electronic sacrificial agent under room temperature[29-31]. It was a two-component photocatalytic hydrogen production system without extra photosensitizer. The volume of H_2 was quantified at the end of the photolysis by gas chromatographic analysis. The optimum pH value of the reaction mixture was maintained at 12.0 (Fig.8a), decreasing or increasing the pH value both resulted in a lower initial rate and shorter system lifetime for hydrogen evolution. The decrease of the efficiency at higher pH values was likely due to the lower concentration of proton in solution. The optimal concentration of NEt_3 is 5%(*V*/*V*) when fixing the pH of the system at the optimum value of 12.0 (Fig.8b). It was mainly because the high concentration of electron sacrificial agents would accelerate the decomposition of photosensitizers. Under optimal conditions, Co-L3 was highly active for the evolution of H_2, the produced hydrogen volume exhibited a linear relationship with the catalyst concentration in a range of 10.0 to 100.0 μmol·L^{-1} (Fig.8c) and the calculated turnover number (TON) was approximately 80. In addition, hardly any observable amount of hydrogen was detected in the dark or in the absence of Co-catalyst under the measured conditions, which showed that Co-catalyst

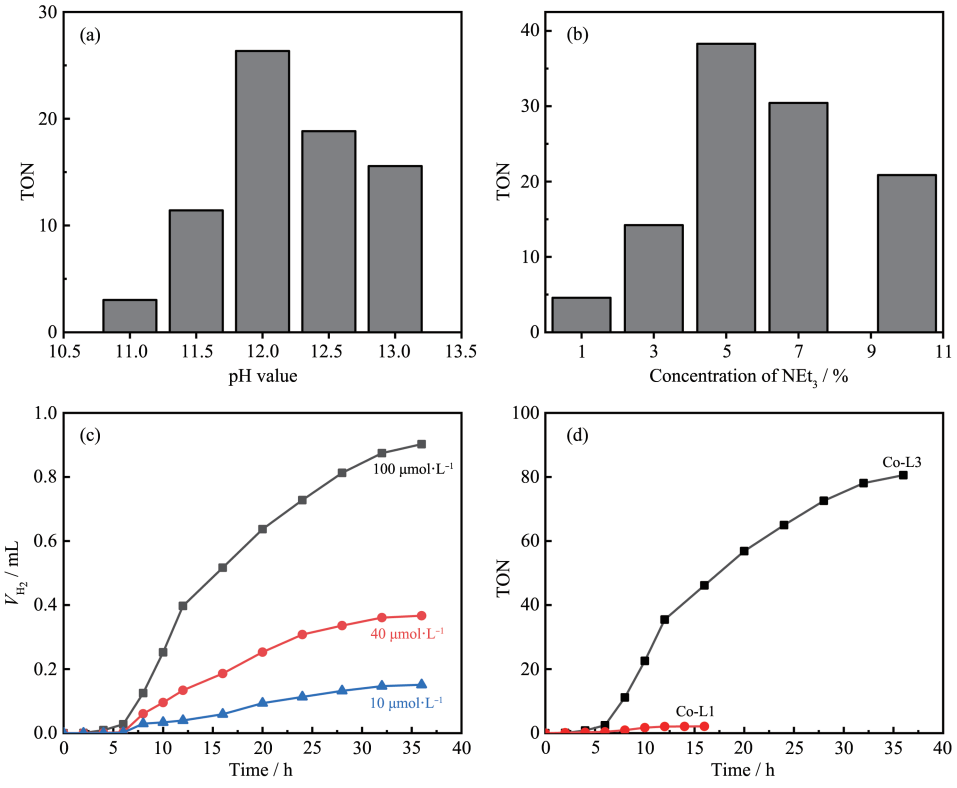

Fig.8 (a) Light-driven H_2 evolution of systems containing Co-L3 (40 μmol·L^{-1}) and NEt_3 (5%, *V*/*V*) in EtOH/H_2O solutions (1∶1, *V*/*V*) with different pH values; (b) Light-driven H_2 evolution of systems containing Co-L3 (40 μmol·L^{-1}) in EtOH/H_2O solution (1∶1, *V*/*V*) at pH=12.0 with different concentrations of NEt_3; (c) Light-driven H_2 evolution of systems containing NEt_3 (5%, *V*/*V*) in EtOH/H_2O solutions (1∶1, *V*/*V*) at pH=12.0 with various concentrations of Co-L3; (d) Light-driven H_2 evolution in EtOH/H_2O (1∶1, at pH=12.0 of three-component system containing Co-L1 (100 μmol·L^{-1}), Fl (100 μmol·L^{-1}) and NEt_3 (5%, *V*/*V*), and two-component system containing Co-L3 (100 μmol·L^{-1}) and NEt_3 (5%, *V*/*V*)

was essential for an efficient photochemical reaction.

Furthermore, a system containing Fl (0.6 mmol·L^{-1}), Co-L1 (0.1 mmol·L^{-1}) and NEt_3 (5%, *V*/*V*) in an EtOH/H_2O (1∶1, *V*/*V*) solution was also used for hydrogen generation. The two-component system containing Co-L3 and NEt_3 showed almost 30 times the hydrogen production efficiency of above three-component system (Fig. 8d). From fluorescence quenching experiments, we could infer that Co-L1 exhibited weak host-guest interactions with fluorescein molecule. Besides, hydrogen evolution was maintained over a period of at least 36 hours in two-component systems containing Co-L3, indicating the introduction of FITC extended the system lifetime for hydrogen production (Fig. 8c). In a word, this artificial photosynthetic system works well in the absence of the Fl, demonstrating that post-assembly modification strategy is an effective and feasible way for the hydrogen generation.

3 Conclusions

In summary, a new post-assembly strategy for constructing artificial photocatalytic systems to generate hydrogen from water by combining an organic photosensitizer FITC with a redox active metal-organic macrocycle was reported. New synthesized metal complexes Co-L3 act as both transition metal catalysts and photosensitizers that capture light energy, hence becoming a two-component hydrogen evolution system without extra photosensitizers. This work may provide a new idea for post-assembly strategy of supramolecular systems in hydrogen production.

References:

[1] Lewis N S, Nocera D G. *Proc. Natl. Acad. Sci. USA.*, **2006**, **103**:15729-15735

[2] Du P W, Knowles K, Eisenberg R. *J. Am. Chem. Soc.*, **2008**, **130**:12576-12577

[3] Liu G, Yin L C, Wang J Q, et al. *Energy. Environ. Sci.*, **2012**, **5**:9603-9610

[4] Wang W Y, Wang H, Zhu Q J, et al. *Angew. Chem. Int. Ed.*, **2016**,**55**:9229-9233

[5] Wang Q, Hisatomi T, Jia Q X, et al. *Nat. Mater.*, **2016**,**15**:611

[6] Meng Q Y, Zhong J J, Liu Q, et al. *J. Am. Chem. Soc.*, **2013**, **135**:19052-19055

[7] Chen B, Wu L Z, Tung C H. *Acc. Chem. Res.*, **2018**,**51**:2512-2523

[8] Chai Z G, Zeng T T, Li Q, et al. *J. Am. Chem. Soc.*, **2016**,**138**:10128-10131

[9] Liu H, Xu C Y, Li D D, et al. *Angew. Chem. Int. Ed.*, **2018**, 57:5379-5383

[10]Kataoka Y, Sato K, Miyazaki Y, et al. *Energy Environ. Sci.*, **2009**,**2**:397-400

[11]Lazarides T, Delor M, Sazanovich I V, et al. *Chem. Commun.*, **2014**,**50**:521-523

[12]Dempsey J L, Brunschwig B S, Winkler J R, et al. *Accounts Chem. Res.*, **2009**,**42**:1995-2004

[13]Khnayzer R S, Thoi V S, Nippe M, et al. *Energy Environ. Sci.*, **2014**,**7**:1477-1488

[14]Martindale B C M, Hutton G A M, Caputo C A, et al. *J. Am. Chem. Soc.*, **2015**,**137**:6018-6025

[15]Dong X Y, Zhang M, Pei R B, et al. *Angew. Chem. Int. Ed.*, **2016**,**55**:2073-2077

[16]Lazarides T, McCormick T, Du P, et al. *J. Am. Chem. Soc.*, **2009**,**131**:9192-9194

[17]Hartley C L, DiRisio R J, Screen M E, et al. *Inorg. Chem.*, **2016**,**55**:8865-8870

[18]Porcher J P, Fogeron T, Gomez-Mingot M, et al. *Angew. Chem. Int. Ed.*, **2015**,**54**:14090-14093

[19]He H Y, Lin J H, Fu W, et al. *Adv. Energy Mater.*, **2016**,**6**:1600464

[20]Kong L Q, Ji Y J, Dang Z Z, et al. *Adv. Funct. Mater.*, **2018**, **28**:1800668

[21]Wang B, He S, Feng W H, et al. *Appl. Catal. B*, **2018**,**236**:233-239

[22]Jing X, Wu P Y, Liu X, et al. *New J. Chem.*, **2015**,**39**:1051-1059

[23]Cai J K, Zhao L, Wei J W, et al. *Chem. Commun.*, **2019**,**55**:8524-8527

[24]Jing X, He C, Yang Y, et al. *J. Am. Chem. Soc.*, **2015**,**137**:3967-3974

[25]Zhao L, Wei J W, Zhang F L, et al. *RSC Adv.*, **2017**,**7**:48989-48993

[26]Yang L, He C, Liu X, et al. *Chem. Eur. J.*, **2016**,**22**:5253-5260

[27]Luo D, Zhou X P, Li D. *Angew. Chem. Int. Ed.*, **2015**,**54**:6190-6195

[28]Wu K, Li K, Chen S, et al. *Angew. Chem. Int. Ed.*, **2019**,**58**:1-6

[29]YANG Lin-Lin(杨林林), JING Xu(景旭), HE Cheng(何成), et al. *Chinese J. Inorg. Chem.*(无机化学学报), **2017**,**33**(6):913-922

[30]JING Xu(景旭), YANG Lin-Lin(杨林林), CHANG Zhi-Duo(常智舵), et al. *Chinese J. Inorg. Chem.*(无机化学学报), **2015**,**31**(5):975-980

[31]LI He-Chuan(李和川), LI Ming-Feng(李明凤), HE Cheng(何成), et al. *Chinese J. Inorg. Chem.*(无机化学学报), **2018**, **34**(1):11-19